American Mineralogist, Volume 66, pages 980–984, 1981

Vapor deposits on olivine in vugs in a basalt: an SEM application

JACQUELINE M. LLOYD[1]

Department of the Geophysical Sciences
The University of Chicago
Chicago, Illinois 60637

Abstract

Vugs in basalt from Hat Creek Valley, California are lined with subhedral to euhedral crystals of plagioclase, pyroxene, olivine and magnetite. The olivines reveal two surface features: rows of platelets (hematite?) and thin films coating the entire olivine crystal surfaces. The presumed hematite platelets are perpendicular to the direction of the rows and are parallel to the (100) plane to the underlying olivine. The rows lie in the (001) plane. It is probable that both the platelets and the thin films are the result of vapor condensation. There may be a structural control between the olivine crystals and the hematite platelets that cause their arrangement parallel to the (100) plane of the olivines and the arrangement of the rows in the (001) plane. Structural control could also explain the absence of these features (except occasionally on plagioclase) on other vug minerals.

Introduction

The rock described in this paper is from a recent subalkaline basalt in Hat Creek Valley, California. The Hat Creek basalt is described by C. A. Anderson (1940) and A. T. Anderson (1971). The sample studied (HC4–12) is from a flow unit located 4 m above the base of a 12 m-high natural cliff and marginal to the main lava river. The rock contains many vesicles lined with well-formed plagioclase, pyroxene, and olivine cyrstals. Regular crystals found lining vesicles are commonly inferred to be vapor deposits (Iddings, 1909, Hatch, *et al.*, 1949, McKay, *et al.*, 1972, Clanton, *et al.*, 1973, Grossman, *et al.*, 1975). The olivine crystals have a bronzy sheen. They were found to have both a thin film coating and rows of crystalline material on their surfaces, which I refer to as "surface deposits" with no genetic implication intended. SEM observation of these surface deposits is the focus of this investigation.

Methods

Two chips from the HC4-12 basalt sample were vacuum-coated with gold-palladium and then studied with a scanning electron microscope and an energy dispersive X-ray detector. Qualitative comparisons were made between the X-ray spectra obtained on olivines with and without rows of surface deposits and thin film coatings. Comparisons were made for plagioclase with and without surface deposits. Individual olivine grains were removed from the vugs and immersed in various acids (HCl, HNO_3, H_2SO_4; all at room temperature and approximately 5N concentration) to test the solubilities of the surface deposits.

In order to determine the crystallographic direction of the rows of surface deposits, I examined olivine grains from the vugs in refractive index oil with a crushing stage. Some of the fractured fragments of olivine retained crystal faces having rows of surface deposits. This made it possible to find the relationship between crystallographic directions in the olivines and the orientation of the rows of surface deposits without encountering interference from the thin films coating the olivine surfaces.

Results

The olivines have indices equal to those for a Fo_{64} olivine (Tröger, 1956): $\alpha = 1.71$, $\beta = 1.73$, and $\gamma = 1.75$. The rows of surface deposits on the olivines are dark brown to opaque. Figure 1 (all figures are SEM photographs) shows an olivine crystal which has two sets of rows of surface deposits typical of vug oli-

[1] Present address: Department of Geology, Florida State University, Tallahassee, Florida 32306.

0003–004X/81/0910–0980$02.00

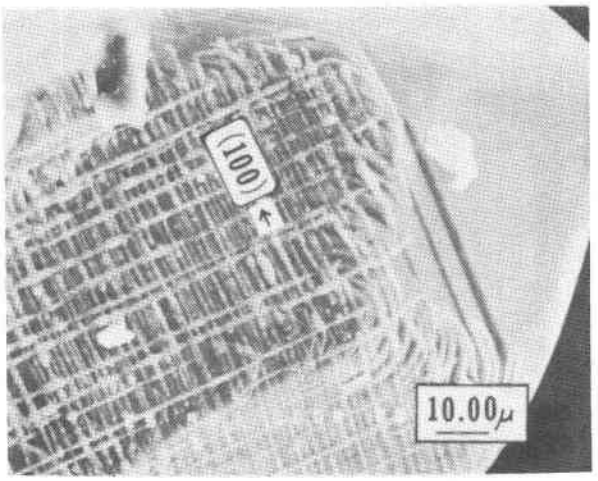

Fig. 1. The two sets of rows of surface deposits are perpendicular to each other. One set is more widely spaced than the other and is not found on all olivine crystals. The closely spaced rows of surface deposits lie in the (001) plane of the underlying olivine and are found on all olivines observed in the HC4-12 sample.

vines. The two sets of rows of surface deposits are perpendicular to each other. One set is more widely spaced than the other and is not found on all olivine crystals. The more closely spaced rows of surface deposits occur on all olivine crystals observed in the HC4-12 sample and are found on most crystal faces. As shown in Figure 1, the closely spaced rows of surface deposits lie in the (001) plane of the underlying olivine. The width of the rows and the distance between the rows varies on individual crystals.

Figure 2a shows both sets of rows of surface deposits. In addition, there are arcuate rows of surface deposits at the rounded edge of two crystal faces. There is also an outer layer of material coating the olivine grain. At the center of the right edge of Figure 2a, are rows of surface deposits which end near where the outer layer has partially peeled away. There is also a peeled portion near the lower left margin of the picture. (See arrows, Figure 2a)

Figures 2b andf 2c are higher magnifications of Figure 2a. Figure 2b reveals that some of the crystal faces are stepped. The rows of surface deposits leading up the edge of the stepped faces curve whereas

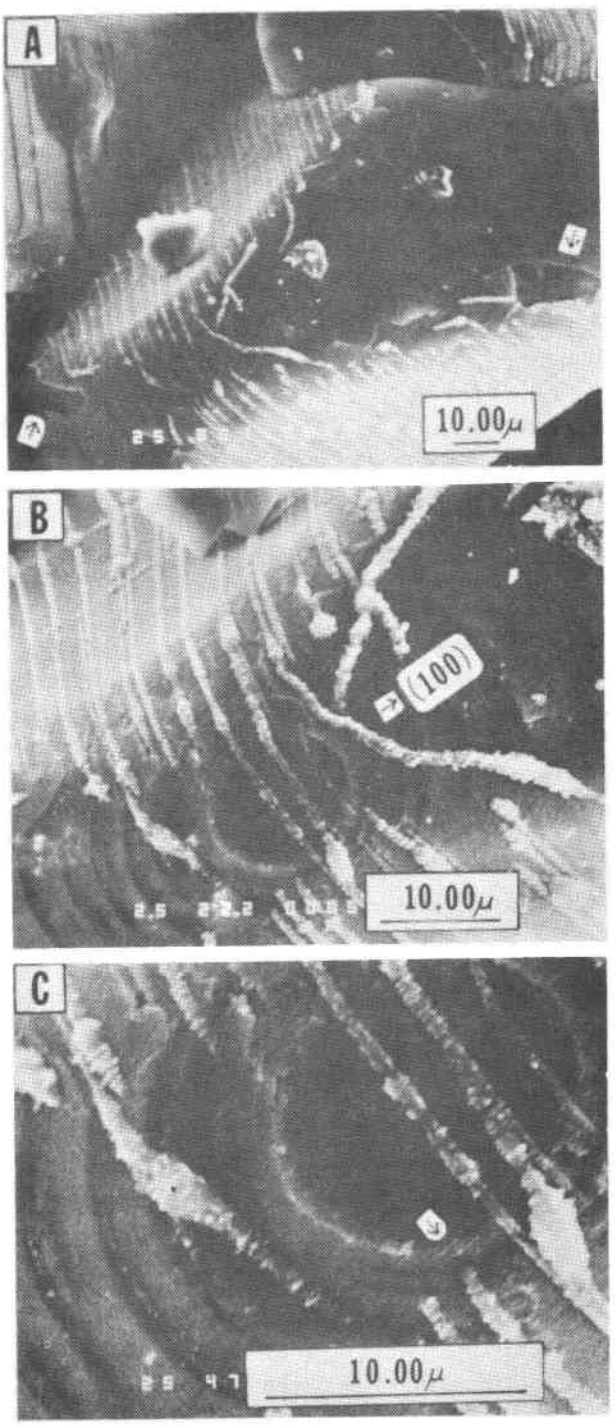

Fig. 2. (a) In addition to the two perpendicular sets of rows of surface deposits, arcuate rows of surface deposits occur at the intersection of two crystal faces. A thin film also coats the crystal. Arrows indicate places where this coating has peeled away. (b) Higher magnification of olivine crystal shown in (a). Individual plates make up the rows of surface deposits and are at a high angle to the underlying olivine surface. Although the rows of surface deposits have various orientations, the individual plates within these rows are all parallel to each other. It appears that these plates are parallel to the (100) plane of the underlying olivine. (c) Higher magnification of the same crystal showing streaking of the thin film coating parallel to the individual plates in the rows of surface deposits.

the rows on adjacent faces continue across the central portion. Individual plates make up the rows of surface deposits and are at a high angle to the underlying olivine surface. Although the rows of surface deposits have various orientations the individual plates within these rows are all parallel to each other. It appears that the plates are parallel to each other and to the (100) plane of the olivine. In Figure 2c the outer coating is observed at higher magnification revealing lineations parallel to the plates of the surface deposits.

Figure 3 shows two adjacent olivine crystals. The rows of surface deposits are oriented with respect to the individual underlying olivine crystal and are not continuous from one grain to an adjacent one.

Surface deposits are rare and irregular on other minerals in the vugs. Figure 4a shows a typical contact between olivine and plagioclase crystals. A line of surface deposit (marked by arrows) follows the junction between the olivine and plagioclase and continues to follow a crack in the plagioclase surface. Figure 4b is a photograph of an olivine grain with a stepped plagioclase crystal in the background. Here a line of surface deposit (marked by arrows) follows the edge of a step in the plagioclase. Both Figures 4a and 4b show typical occurrences of the rows of surface deposits on plagioclase. Structural control breaks down as the boundary between olivine and plagioclase is crossed. Some surface deposits also occur as single aggregates (not shown), approximately 3 μ in diameter, on plagioclase.

The qualitative X-ray energy dispersive analysis revealed that the rows of surface deposits and the thin film coatings are Fe-enriched compared to the underlying olivine and plagioclase crystals. There is also some increase in the amount of Ca and Mn observed for most of the analyses. A few analyses also showed a slight increase in the amount of Cu. The rows of surface deposits and the thin film coatings are insoluble in HCl, HNO_3, and H_2SO_4 at room temperature and approximately 5N concentration.

Discussion

The surface deposits on the olivines are probably the result of condensation from a vapor phase. This process is consistent with the common inference that regular crystals in vugs condense from a vapor (Iddings, 1909, Hatch, *et al.*, 1949, McKay, *et al.*, 1972, Clanton, *et al.*, 1973, Grossman, *et al.*, 1975). The Fe-rich composition of the surface deposits suggests that they consist of Fe oxides, which are known to occur as vapor condensates in volcanic rocks (Zies, 1924, Krauskopf, 1957, Mizutani, 1962, Martin, *et al.*, 1969).

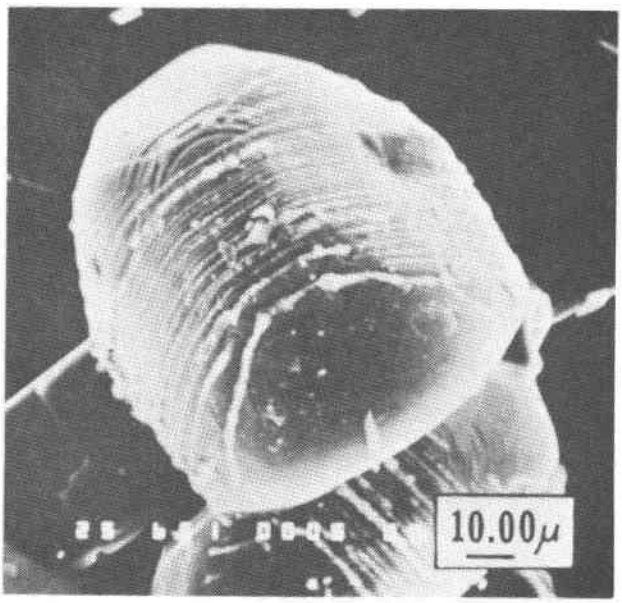

Fig. 3. Two adjacent olivine crystals showing oriented pattern of the rows of surface deposits. The direction of rows of surface deposits is not continuous across olivine grain boundaries, but is specific to the individual grain it is associated with.

The probable enrichment of Ca, Mn, and some Cu in the rows of surface deposits is likewise consistent with volcanic vapors and condensates. These elements are considered to be transported as chlorides, fluorides, sulfides, or carbonates (Murata, 1960, Mitzutani, 1972). Alkalies and iron are often observed in volcanic flames (Krauskopf, 1957, Martin, *et al.*, 1969, Mizutani, 1972) and CuCl has been observed at the 1960 Kilauea eruption (Murata, 1960) and also at Nyiragongo Volcano in Africa (Delsemme, 1960).

Mizutani (1962) describes a model for the formation of fumerolic hematite as a vapor condensate. As the temperature of the gas decreases magnetite is first deposited. Magnetite is subsequently oxidized by atmospheric oxygen to form hematite. Alternatively, crystals of hematite can be formed directly from a vapor phase by reacting ferric chloride with a source of oxygen at a high temperature.

Further consideration of the Fe oxide as a vapor deposit requires an explanation for the structural relationship between the presumed Fe oxide and the olivine crystals. Roedder (1971) observed ilmenite as daughter crystals in olivine in lunar samples. The plates of ilmenite are arranged parallel to the (100) plane of the enclosing olivine. He also found that by melting and then slowly cooling melt inclusions in

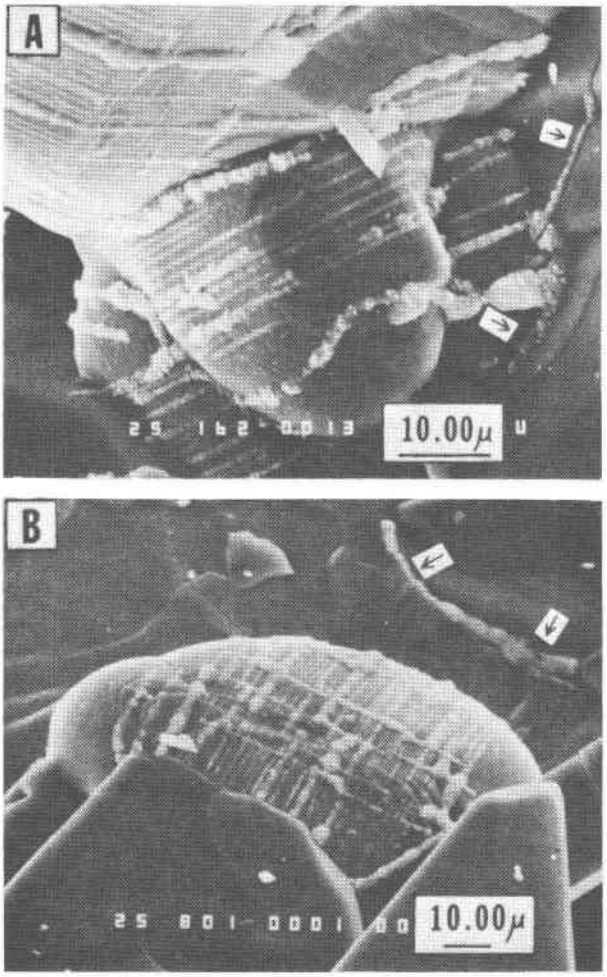

Fig. 4. (a) Typical contact between olivine and plagioclase crystals. A line of surface deposit follows the junction between an olivine and plagioclase and continues to follow a crack in the plagioclase surface. (b) Olivine grain with a stepped plagioclase crystal in the background. The surface deposit on the plagioclase follows the edge of a step. Box (a) and (b) demonstrate the breakdown of structural control as grain boundaries between olivine and plagioclase are crossed.

olivine in some Hawaiian lava lake samples, thin plates of ilmenite crystals reformed, parallel to (100) of the host olivine. Similar oriented growth of ilmenite plates around the outside of olivine phenocrysts was observed by Drever and Johnston (1957). They attributed these relationships to either (1) intergrowth and/or overgrowth of ilmenite on the olivine substrate or (2) ilmenite replacement of lateral branches of previously dendritic olivine.

Qualitative chemical analyses do not show any Ti present in the rows of surface deposits, so they are probably not composed of ilmenite. Insolubility in acid eliminates Fe oxides such as goethite. Other possibilities are magnetite and hematite. The platy morphology suggests hematite rather than magnetite.

Hematite is trigonal and contains alternating layers of oxygen and iron ions perpendicular to the triad axis. The oxygen ions are in slightly distorted hexagonal packing (Deer, *et al.*, 1966). Since the olivine structure also contains hexagonally packed oxygen ions, in sheets parallel with the (100) plane, condensation of hematite onto olivine crystals might be favored since oxygen layers would match with the underlying olivine.

Conclusions

The above observations and reasoning suggest the following model. The surface deposits on the olivines condensed from an Fe-bearing gas as hematite. The preferred occurrence of the rows of surface deposits on olivines is due to structural compatability between olivine and hematite (plates of probable hematite with (0001) parallel to (100) of the underlying olivine). The reason for rows lying predominately in the (001) plane of the olivine is not clear.

Acknowledgments

A. T. Anderson advised and guided me throughout this research. A. T. Anderson, W. C. Parker, J. V. Smith, and S. E. McLeese read the original manuscript and suggested improvements. E. Roedder reviewed the manuscript and provided useful criticism. Paul Moore and I discussed the epitaxial growth of hematite and olivine. Paul Moore also took X-ray photographs of several olivine crystals. Thin sections of rocks studied were provided by A. T. Anderson. Dennis Cassidy assisted in making the plates for the figures. The research was supported in part by NSF Grant EAR 76-15016 (to A. T. Anderson) and by NSF Grant EAR 77-27100 and NASA Grant 14-001-171 (to J. V. Smith).

References

Anderson, A. T. (1971) Alkali-rich, SiO_2-deficient glasses in high-alumina olivine tholeiite, Hat Creek Valley, California. American Journal of Science, 271, 293–303.

Anderson, C. A. (1940) Hat Creek lava flow. American Journal of Science, 238, 477–492.

Clanton, U. S., McKay, D. S., and Ladle, G. H. (1973) Scanning electron microscopy of lunar material. JEOL News, 11e, 2-9.

Deer, W. A., Howie, R. A., and Zussman, J. (1966) An Introduction to the Rock Forming Minerals. Longman Group Limited, London.

Delsemme, A. H. (1960) Spectroscopie de flammes volcaniques. Académie Royale des Sciences d'outre-mer, Bulletin des Séances, Bruxelles, New Series, 6, 507–519.

Drever, H. I. and Johnston, R. (1957) Crystal growth of forsteritic olivine in magmas and melts. Transactions of the Royal Society of Edinburgh, 63, 289–315.

Grossman, L., Fruland, R. M., and McKay, D. S. (1975) Scanning electron microscopy of a pink inclusion from the Allende meteorite. Geophysical Research Letters, 2, 37–40.

Hatch, F. H., Wells, A. K., and Wells, M. K. (1949) The Petrology of the Igneous Rocks. Thomas Murby and Co., London.

Iddings, J. P. (1909) Igneous Rocks. John Wiley & Sons, N. Y., Chapman & Hall, Ltd., London.

Krauskopf, K. B. (1957) The heavy metal content of magmatic vapor at 600°C. Economic Geology, 52, 786–807.

Martin, R. F. and Piwinskii, A. J. (1969) Experimental data bearing on the movement of iron in an aqueous vapor. Economic Geology, 64, 798–803.

McKay, D. S., Clanton, U. S., Morrison, D. A., and Ladle, G. H. (1972) Vapor phase crystallization in Apollo 14 breccia. Geochimica Cosmochimica Acta, 36, Supplement 3, 739–752.

Mizutani, Y. (1972) Volcanic sublimates and incrustations from Showashinzan. The Journal of Earth Science, Nagoya University, 10, 149–164.

Murata, K. J. (1960) Occurrence of CuCl emission in volcanic flames. American Journal of Science, 258, 769–772.

Roedder, E. (1971) Natural and laboratory crystallization of lunar glasses from Apollo 11. Mineral Society of Japan, Special Paper, 1, 5–12.

Tröger, W. E. (1956) Optische Bestimmung der Gesteinsbildenden Minerale, Teil 1, Bestimmungstabellen. E. Schweizer-bart'sche Verlagsbuchhandlung, Stuttgart W.

Zeis, E. G. (1924) The fumerolic incrustations in the Valley of Ten Thousand Smokes. National Geographic Society Contributed Technical Papers, Katmai Series, 1, 157–179.

Zeis, E. G. (1929) The Valley of Ten Thousand Smokes, pt 1, fumerolic incrustations and their bearing on ore deposition. National Geographic Society Contributed Technical Papers, Katmai Series, 1, number 4.

Manuscript received, April 27, 1979;
accepted for publication, April 28, 1981.